



## Vibrational Spectroscopy

Elixir Vib. Spec. 52 (2012) 11425-11436

Elixir  
ISSN: 2229-712X

# Vibrational spectra, NBO, HOMO-LUMO and NMR ( $^1\text{H}$ and $^{13}\text{C}$ ) analyses of 5-bromo-2-methoxybenzaldehyde

V. Balachandran<sup>1,\*</sup> and G. Santhi<sup>2</sup>

<sup>1</sup>Department of Physics, A A Government Arts College, Musiri, Tiruchirappalli 621211, India.

<sup>2</sup>Department of Physics, Government Arts College, Karur 639005, India.

### ARTICLE INFO

#### Article history:

Received: 1 July 2012;

Received in revised form:

12 November 2012;

Accepted: 14 November 2012;

#### Keywords

Vibrational spectra,  
DFT,  
5-bromo-2-methoxybenzaldehyde,  
HOMO-LUMO,  
NMR.

### ABSTRACT

In this work, the spectral properties of 5-bromo-2-methoxybenzaldehyde (BMB) are studied using density functional theory (DFT) employing B3LYP/6-311++G (d) and B3LYP/6-311++G (d, p) levels of theory. There are four conformers, C1, C2, C3, and C4 for this molecule. The computational results diagnose the most stable conformer of BMB as the C1 form. The optimized geometrical parameters obtained by B3LYP/6-311++G (d, p) method show good agreement with experimental X-ray data. The electric dipole moment ( $\mu$ ) and first hyperpolarizability ( $\beta$ ) values of the investigated molecule are computed using scaled quantum mechanics (SQM) method. The calculated results also show that the BMB might have microscopic non-linear optical (NLO) behavior with non-zero values. A study on the electronic properties, such as HOMO and LUMO energies, is performed. The isotropic chemical shift computed by  $^1\text{H}$  and  $^{13}\text{C}$  nuclear magnetic resonance (NMR) chemical shifts of the BMB calculated using the gauge invariant atomic orbital (GIAO) method also shows good agreement with experimental observations.

© 2012 Elixir All rights reserved.

### 1. Introduction

5-Bromo-2-methoxybenzaldehyde is an aromatic aldehyde with methoxy group. It is soluble in alcohol and ether, but it is insoluble in water. It is used in the synthesis of other organic compounds including pharmaceuticals (especially antihistamines), agrochemicals, dyes and plastic additives. It is an important intermediate for the processing of perfumes and flavoring compounds [1].

Extensive experimental and theoretical investigations have focused on elucidating the structure and normal vibrations of benzaldehyde derivatives. Vibrational assignment based FT-IR and Raman spectra and theoretical DFT calculations have been studied for benzaldehyde derivatives [2–6]. Gunasekaran *et al.* [7] investigated vibrational modes of p-methoxybenzaldehyde by both experimental as well as theoretical methods; however, literature survey reveals that to the best of our knowledge, no experimental and computational vibrational spectroscopic study on free BMP is published in the literature yet. This inadequacy observed in the literature encouraged us to make this theoretical and experimental vibrational spectroscopic research based on the conformers of BMB to give a correct assignment of the fundamental bands in experimental FT-IR and FT-Raman spectra. Therefore, present study aims to give a complete description of the molecular geometry and molecular vibrations of the BMB. The possible stable conformers of BMB are searched. The optimized geometry and vibrational frequencies for the C1 stable conformer of BMB are calculated at DFT/B3LYP level of theory using the 6-311++G (d) and 6-311++G (d, p) basis sets. The results of the theoretical and spectroscopic studies are reported herein. These calculations are valuable for providing insights into the vibrational spectrum and molecular parameters. A detailed interpretation of the

vibrational spectra of BMB has been made on the basis of the calculated potential energy distribution (PED).

The calculated HOMO (highest occupied molecular orbital) and LUMO (lowest unoccupied molecular orbital) energies show that charge transfer occurs in BMB. Density functional theory calculations are reported to provide excellent vibrational frequencies of organic compounds if the calculated frequencies are scaled to compensate for the approximate treatment for electron correlation, for basis set deficiencies and for the anharmonicity [8–9].

### 2. Experimental Details

The sample BMB was provided by the Lancaster Chemical Company, (UK), with a purity of greater than 98%, and it was used as such without further purification. The room temperature FT-IR spectrum of BMB was recorded in the frequency region 400–4000  $\text{cm}^{-1}$  at a resolution of  $\pm 1 \text{ cm}^{-1}$  using BRUKER IFS 66V FTIR spectrometer equipped with an MCT detector, a KBr beam splitter and globar source. The FT-Raman spectrum of BMB was recorded on a computer interfaced BRUKER IFS 66V model interferometer equipped with FRA-106 FT-Raman accessories. The spectrum was measured in the Stokes region 3500–100  $\text{cm}^{-1}$  using Nd: YAG laser at 1064 nm of 200 mW output as the excitation source and with a liquid nitrogen-cooled Ge-diode detector with the powder sample in a capillary tube. 1000 scans were accumulated to increase the signal-to-noise ratio with a total registration time of about 30 min. The reported wave numbers are expected to be accurate within  $\pm 1 \text{ cm}^{-1}$ . A correction according to the fourth-power scattering factor was performed, but no instrumental correction was made.  $^1\text{H}$  and  $^{13}\text{C}$  nuclear magnetic resonance (NMR) (400 MHz;  $\text{CDCl}_3$ ) spectra were recorded on a BRUKER HC400 instrument.

Chemical shifts for protons are reported in parts per million scales (d scale) downfield from tetramethylsilane.

### 3. Computational Details

In order to obtain stable structures, the geometrical parameters for C1 conformer of BMB in the ground state were obtained at DFT by the B3LYP level of theory using the 6-311++G (d) and 6-311++G (d, p) basis sets. Moreover, the vibrational wavenumbers of BMB conformation have also been calculated to improve simulation of the experimental spectra. The computed bond lengths and bond angles by both levels show satisfactory agreement with experimental [7] observation. We tabulated only C1 conformer calculations that are performed using Gaussview molecular visualization program [10] and Gaussian 09W program package on the personal computer [11].

The Becke's three-parameter hybrid density functional, B3LYP [12–13], was used to calculate harmonic vibrational wavenumbers with 6-311++G (d) and 6-311++G (d, p) basis sets. It is well known in the quantum chemical literature that among available B3LYP function yields a good description of harmonic vibrational wavenumbers for small and medium-sized molecules.

Natural bond orbital analysis was also performed by the Gaussian 09W program at the B3LYP level of theory analysis which transforms the canonical delocalized Hartree–Fock (HF) molecular orbital (MOs) into localized MOs that are closely tied to chemical bonding concepts. This process involves sequential transformation of non-orthogonal atomic orbitals (AOs) to the sets of natural atomic orbital (NAO), natural hybrid orbital (NHO) and NBO. Natural bond orbital analysis gives the accurate possible natural Lewis structure picture of orbital because all orbital are mathematically chosen to include the highest possible percentage of the electron density. Interaction between both filled and virtual orbital spaces information correctly is explained by the NBO analysis, and it could enhance the analysis of intra- and intermolecular interactions. The interaction between filled and antibonding orbital represents the deviation of the molecule from the Lewis structure and can be used as the measure of delocalization. This non-covalent bonding–antibonding charge transfer interactions can be quantitatively described in terms of the second-order perturbation interaction energy  $E^{(2)}$  [15]. This energy represents the estimate of the off-diagonal NBO Fock matrix elements. It can be deduced from the second-order perturbation approach [16] as follows:

$$E^{(2)} = \Delta E_{ij} = q_i \frac{F_{(i,j)}^2}{\varepsilon_j - \varepsilon_i}$$

where  $q_i$  is the  $i$ th donor orbital occupancy,  $\varepsilon_j$  and  $\varepsilon_i$  are diagonal elements (orbital energies) and  $F(i, j)$  is the off-diagonal NBO Fock matrix element.

### 4. Hyperpolarizability

The first hyperpolarizability ( $\beta$ ) of this novel molecular system and related properties ( $\beta$ ,  $\alpha$ , and  $\Delta\alpha$ ) of BMB were calculated using B3LYP/6-311++G (d, p) basis set, based on the finite-field approach. In the presence of an applied electric field, the energy of system is the function of the electric field. Polarizability and hyperpolarizability characterize the response of a system in an applied electric field [17]. They determine not only the strength of molecular interactions (long-range interinduction, dispersion force, etc.) and the cross sections of different scattering and collision process but also the non-linear optical properties (NLO) of the system [18, 19]. First

hyperpolarizability is a third-rank tensor that can be described by  $3 \times 3 \times 3$  matrix. The 27 components of the 3D matrix can be reduced to 10 components due to the Kleinman symmetry [20]. It can be given in the lower tetrahedral format. It is obvious that the lower part of the  $3 \times 3 \times 3$  matrixes is a tetrahedral. Components of  $\beta$  are defined as coefficients in the Taylor series expansion of the energy in the external electric field. When the external electric field is weak and homogeneous, this expansion becomes as follows:

$$E = E^0 - \frac{\mu_i F_i}{1!} - \frac{\alpha_{ij} F_i F_j}{2!} - \frac{\beta_{ijk} F_i F_j F_k}{3!} - \frac{\gamma_{ijkl} F_i F_j F_k F_l}{4!} + \dots$$

where  $E^0$  is the energy of the unperturbed molecules,  $F_\alpha$  is the field at the origin, and  $\mu_\alpha$ ,  $\alpha_{\alpha\beta}$ , and  $\beta_{\alpha\beta\gamma}$  are the components of dipole moment, polarizability and the first hyperpolarizability respectively.

The total static dipole moment is

$$\mu = (\mu_x^2 + \mu_y^2 + \mu_z^2)^{\frac{1}{2}}$$

The isotropic polarizability is

$$\alpha = \frac{\alpha_{xx} + \alpha_{yy} + \alpha_{zz}}{3}$$

The polarizability anisotropy invariant is

$$\Delta\alpha = 2^{-\frac{1}{2}} [(\alpha_{xx} - \alpha_{yy})^2 + (\alpha_{yy} - \alpha_{zz})^2 + (\alpha_{zz} - \alpha_{xx})^2 + 6\alpha_{xx}^2]^{\frac{1}{2}}$$

$$\beta_{tot} = (\beta_x^2 + \beta_y^2 + \beta_z^2)^{\frac{1}{2}}$$

$$\beta_x = \beta_{xxx} + \beta_{yyy} + \beta_{zzz}$$

$$\beta_y = \beta_{yyy} + \beta_{xxy} + \beta_{yzz}$$

$$\beta_z = \beta_{zzz} + \beta_{xzx} + \beta_{yyz}$$

and the average hyperpolarizability is

$$\beta_{tot} = (\beta_x^2 + \beta_y^2 + \beta_z^2)^{\frac{1}{2}}$$

where  $E$  is the energy of the unperturbed molecules,  $F_i$  is the field at the origin and  $\mu_i$ ,  $\alpha_{ij}$ ,  $\beta_{ijk}$  and  $\gamma_{ijkl}$  are the components of dipole moment, polarizability, first hyperpolarizability and the second hyperpolarizability, respectively. The total static dipole moment  $\mu$ , the mean polarizability  $\alpha$ , the anisotropy of the polarizability ( $\Delta\alpha$ ) and the first hyperpolarizability  $\beta_{tot}$  using the  $x$ ,  $y$  and  $z$  component, are defined. The B3LYP/6-311++G (d, p) calculated the first hyperpolarizability of BMB is  $11.5 \times 10^{-31}$  esu. The total molecular dipole moment ( $\mu$ ), mean polarizability ( $\alpha$ ) and anisotropy polarizability ( $\Delta\alpha$ ) of BMB have been collected in Table 1. When comparing the hyperpolarizability of other molecules reported earlier [21, 22], the value of first hyperpolarizability of BMB molecule possesses non-linear optical properties that can be used for NLO applications.

### 5. Potential energy distribution

To check whether the chosen set of symmetric coordinates contribute maximum to the potential energy associated with the molecule, the PED has been carried out. The vibrational problem was set up in terms of internal and symmetry coordinates. The Cartesian representation of the theoretical force constants has been computed at the fully optimized geometry by assuming Cs point group symmetry. The symmetry of the molecule was also helpful in making vibrational assignment. The transformation of force field, subsequent normal coordinate analysis and calculation of the PED were done on a PC with the MOLVIB program (version V7.0-G77) written by Sundius [23, 24].

## 6. Results and discussion

In the C1, C2, C3 and C4 forms of molecule, BMB and benzene ring are in the same plane. The optimized structures and numbering of the atoms of BMB are shown in Fig. 1. We reported same geometric parameters and vibrational frequencies for BMB using DFT (B3LYP) and compared with the experimental crystal geometries (bond lengths, bond angles) [7] and experimental frequencies.

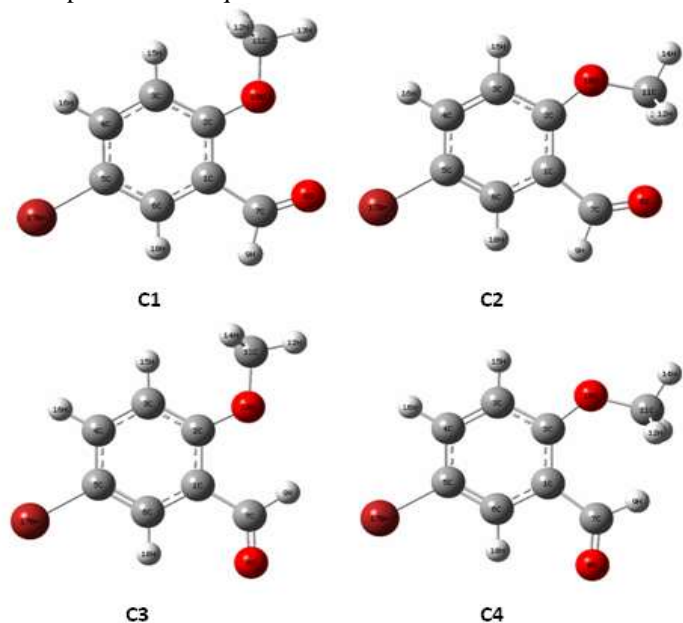


Fig.1. Optimized structures and numbering of the atoms of 5-bromo-2-methoxybenzaldehyde

### 6.1 Energetics

Calculated energies and energy difference for all conformers of BMB determined by B3LYP level with 6-311++G (d) and 6-311++G (d, p) basis sets are presented in Table 2. From DFT calculations using 6-311++G (d, p) basis set, the conformer C1 is predicted to be from 11.5 to 32.54 kJ/mol more stable than the other conformers. As clearly seen from the values given in Table 2, the basis set size effect on the calculated energies is not so much, but of considerable importance; use of the basis sets of larger sizes gives rise to slight increases in the differences; however, unstable conformers give rise to decreases in the differences between the calculated energies.

### 6.2 Geometric structure

The optimized bond lengths, bond angles and dihedral angles of BMB calculated by B3LYP method using B3LYP 6-311++G (d) and 6-311++G (d, p) basis sets are listed in Table 3 in accordance with atom numbering scheme as shown in Fig. 1. Since the exact crystal structure of BMB is not available till now, the optimized structure can only be compared with other similar system [7] for which the crystal structures have been solved. Therefore optimized geometrical parameters of 2-methoxybenzaldehyde are compared to those of BMB. From the theoretical values we can find that most of the optimized bond lengths are slightly larger and shorter than experimental values. Comparing bond lengths and bond angles of C<sub>s</sub> point group symmetry at B3LYP/6-311++G (d, p) method leads to geometric parameters that which are much closer to experimental values.

Several researchers [25, 26] have explained the changes in the frequency or bond length of the C – H bond on substitution due to a change in the charge distribution on the ring carbon atom of the benzene ring. The substituent may be of either the electron-withdrawing type (F, Cl, Br, NO<sub>2</sub>, etc) or electron-

donating type (CH<sub>3</sub>, C<sub>2</sub>H<sub>5</sub>, NH<sub>2</sub>, etc). The carbon atoms are bonded to the hydrogen atoms with  $\sigma$  bond in benzene and substitution of a Br atom for hydrogen reduces the electron density at the ring carbon atom. The ring carbon atoms in substituted benzene exert a large attraction on the valence electron cloud of the hydrogen atom resulting in an increase in the C–H force constant and a decrease in the corresponding bond length which would be influenced by the combined effects on the inductive mesomeric interaction and the electric dipole field of the polar substituent. In this study, the C–H bond lengths were calculated as 1.10 and 1.09 Å for the ring.

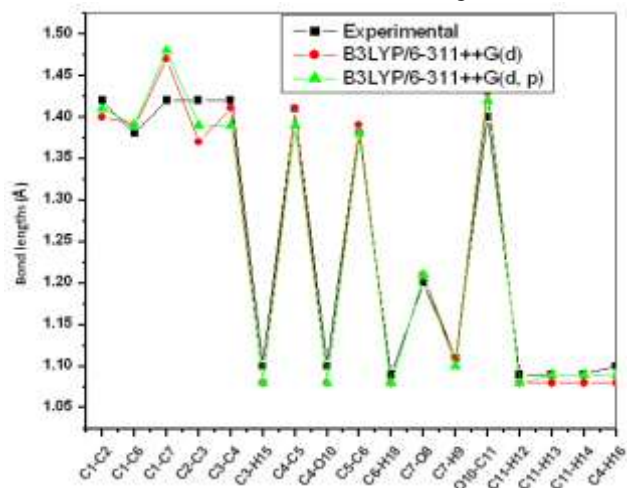


Fig. 2. Bond length differences between theoretical B3LYP/6-311++G (d) and B3LYP/6-311++G (d, p) approaches of the 5-bromo-2-methoxybenzaldehyde

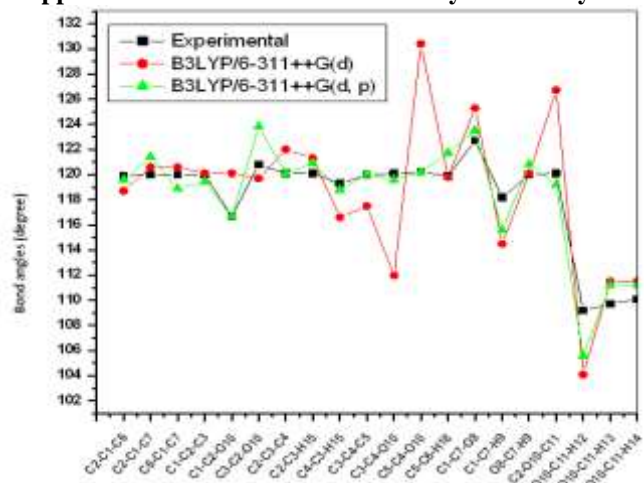


Fig. 3. Bond angle differences between theoretical B3LYP/6-311++G (d) and B3LYP/6-311++G (d, p) approaches of the 5-bromo-2-methoxybenzaldehyde

The optimized parameters obtained by B3LYP method using 6-311++G (d) and 6-311++ G (d, p) basis sets are approximately similar than to those observed experimentally. At all levels reported here, the calculated bond lengths and bond angles are very close to experimental values, except for the angle at the point of substitution. As seen in Table 3, the interaction between the bromine atom and aromatic ring produces a small displacement of the bromine atom out of the benzene ring with a torsion angle of Br17–C5–C4–C6 in ca. 179.9°. However, the trends in the distortion of the benzene ring upon substitution are correct with an electron-donating an electron-withdrawing substituent at the *para* positions, the symmetry of the benzene ring is distorted, yielding ring angles

smaller than  $120^\circ$  at the point of substitution and slightly longer than  $120^\circ$  at the *ortho*- and *meta*- position. The C5–Br17 bond distance is 1.9Å. It is interesting to note that C11–H12, C11–H13 and C11–H14 bond lengths in methyl group are same i.e., 1.09Å.

Normal coordinate analysis is the mathematical procedure that gives the normal coordinates, their frequencies, and force constants. The detailed description of vibrational modes can be given by means of normal coordinate analysis. The internal coordinates describe the position of the atoms in terms of distances, angles and dihedral angles with respect to an origin atom. The symmetry coordinates are constructed using the set of internal coordinates. In this study, the full set of 61 standard internal coordinates (containing 13 redundancies) for BMB was defined as given in Table 4. From these, a non-redundant set of local symmetry coordinates was constructed by suitable linear combinations of internal coordinates which are presented in Table 5.

Comparing bond angles and bond lengths using B3LYP at 6-311++G (d) and 6-311++G (d, p) levels, and the calculated values correlates well compared with the experimental data. Although there are some differences, calculated geometrical parameters represent a good approximation and they are basis for calculating other parameters such as vibrational frequencies and thermodynamic properties. The comparative graphs of bond lengths and bond angles of the BMB using 6-311++G (d) and 6-311++G (d, p) basis sets are given in Figs. 2–3.

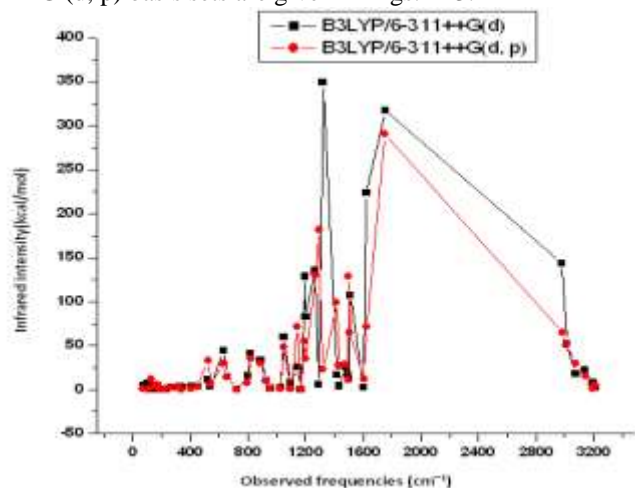


**Fig. 4.** Comparative graph of IR intensities by B3LYP/6-311++G (d) and B3LYP/6-311++G (d, p) for 5-bromo-2-methoxybenzaldehyde

### 6.3 Computed IR intensity and Raman activity analyses

Computed vibrational spectral IR intensities and Raman activities of BMB for corresponding wavenumbers by DFT method at B3LYP with 6-311++G (d) and 6311++G (d, p) basis sets have been listed in Table 6. The comparative graphs of IR intensities and Raman activities and with observed frequency for the basis sets 6-311++G (d) and 6-311++G (d, p) are shown in Figs. 4–5, respectively.

### 6.4 Vibrational spectral analysis

It has been argued that in 5-bromo-2-methoxybenzaldehyde, all the atoms except atoms of CH<sub>3</sub> group are in the same plane. In the present study, C and H atoms of CH<sub>3</sub> group are taken to be in plane of the methyl group. With this assumed structural model, the molecule under consideration would belong to C<sub>s</sub> point group and the 48 normal modes of vibrations which span the irreducible representations: 33A'+15A". The harmonic

vibrational frequencies calculated for BMB at B3LYP level using the 6-311++G (d) and 6-311++G (d, p) basis sets along with reduced mass, force constants, infrared intensities, Raman activities, and depolarization ratio have been summarized in Table 6.

Comparison of the frequencies calculated at B3LYP with experimental values (Table 7) reveals the overestimation of the calculated vibrational modes due to neglect of anharmonicity in real system. Inclusion of electron correlation in density functional theory to a certain extent makes the frequency values smaller in comparison with the 6-311++G (d) data. Figs. 6 and 7 present the experimental and theoretical FT-IR and FT-Raman spectra of BMB, respectively.

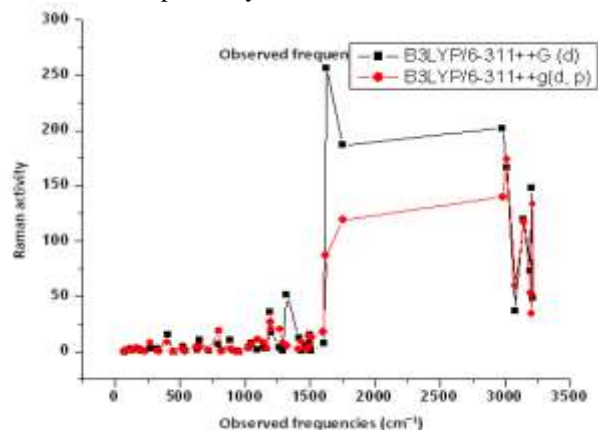


**Fig. 5.** Comparative graph of Raman activity by B3LYP/6-311++G (d) and B3LYP/6-311++G (d, p) for 5-bromo-2-methoxybenzaldehyde

#### 6.4.1 Aldehyde group vibrations

The C–H stretching vibrations of the aldehyde group [27] usually appear in the region 2871–2806 cm<sup>-1</sup>. Hence in the present work, C–H stretching vibration computed by B3LYP/6-311++G (d, p) method at 2902 cm<sup>-1</sup> for BMB shows a very good agreement with recorded value. The weak band observed with the FT-IR spectrum at 2898 cm<sup>-1</sup> and the Raman spectrum at 2900 cm<sup>-1</sup> is assigned to C–H stretching vibration of the aldehyde group. The in-plane C–H deformation mode of aldehyde group is observed at 950 cm<sup>-1</sup> with strong intensity in the FT-IR spectrum for BMB. The carbonyl (C=O) stretching vibrations in the substituted benzaldehydes are reported near 1700 cm<sup>-1</sup> [27]. The very strong band centered 1758 cm<sup>-1</sup> in FT-IR for BMB is attributed to C=O stretching vibration of the aldehyde group. In the present investigation, the medium strong FT-Raman band observed at 803 cm<sup>-1</sup> for BMB could be assigned to C=O in-plane bending vibration. In BMB, the weak band centered at 321 cm<sup>-1</sup> in FT-Raman spectra could be assigned to C=O out-of-plane bending vibrations of aldehyde group. A weak-to-medium intensity band due to the aldehyde group CHO deformation vibration [26] is found in the region 975–780 cm<sup>-1</sup>. In consonance with this, the medium-to-strong intensity band at 884 cm<sup>-1</sup> could be assigned to CHO out-of-plane deformation for BMB.

#### 6.4.2 C–H vibrations

For simplicity, modes of vibrations of aromatic compounds are considered as separate C–H or ring C–C vibrations. However, as with any complex molecules, vibrational interactions occur and these levels only indicate the predominant vibration. Substituted benzenes have large number of sensitive bands, i.e., bands whose position is significantly affected by the

mass and electronic properties, mesomeric or inductive of the substituents. According to the literature [28–29], in infrared spectra, most mononuclear and polynuclear aromatic compounds have three or four peaks in the region  $3000\text{--}3100\text{ cm}^{-1}$ , these are due to the stretching vibrations of the ring CH bands. Accordingly, in the present study, the FT-IR bands identified at 3098, 3048, and  $2998\text{ cm}^{-1}$  and FT Raman bands at 3095, 3054 and  $3002\text{ cm}^{-1}$  are assigned to C–H stretching vibrations of BMB which are in good agreement with calculated values by B3LYP/6-311++G (d, p) 3095, 3052, and  $3006\text{ cm}^{-1}$ . The FT-IR bands at 1468, and  $1396\text{ cm}^{-1}$  and the FT Raman bands at 1487 and  $1395\text{ cm}^{-1}$  are assigned to C–H in-plane bending vibration of BMB. The C–H out-of-plane bending vibrations of the BMB are well identified at 1239, and 908 and  $1184\text{ cm}^{-1}$  in the FT-IR and  $1184\text{ cm}^{-1}$  in the FT-Raman spectra which are found to be well within their characteristic region.

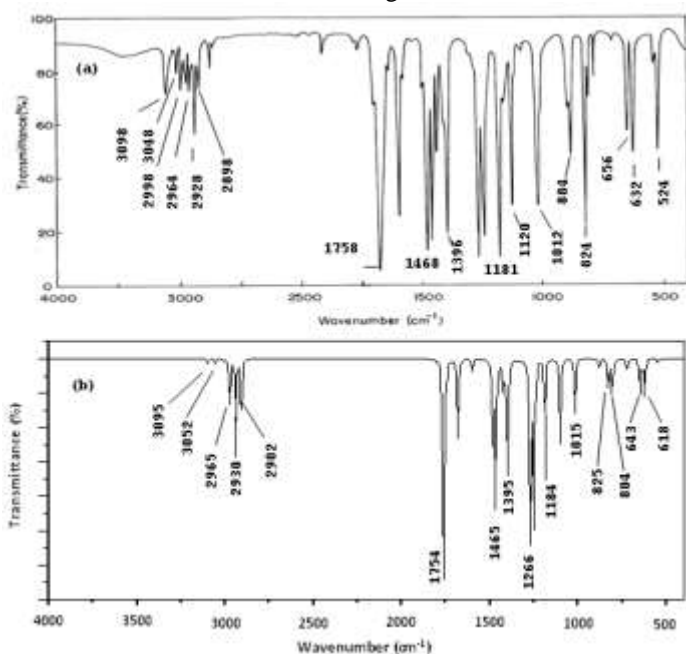


**Fig. 6.** FTIR spectrum of 5-bromo-2-methoxybenzaldehyde (a) Observed (b) Calculated by B3LYP/6-311++G(d,p)

#### 6.4.3 C–C vibrations

The ring C=C and C–C stretching vibrations, known as semicircle stretching usually occur in the region  $1400\text{--}1625\text{ cm}^{-1}$  [30–31]. Hence in the present investigation, the FT-IR bands identified at 1690, 1432, and 1264 and  $1120\text{ cm}^{-1}$  and the FT-Raman bands at 1671, 1276, 1118 and  $1092\text{ cm}^{-1}$  are assigned to C–C stretching vibrations of BMB. The band ascribed at  $716\text{ cm}^{-1}$  in FT-IR and  $412\text{ cm}^{-1}$  in FT-Raman spectra has been designated to CC in-plane and out-of-plane bending mode. The calculated bending modes found at  $715\text{ cm}^{-1}$  and  $410\text{ cm}^{-1}$  in B3LYP/6-311++G (d, p) are assigned to C–C in-plane and out-of-plane bending vibrations, respectively.

#### 6.4.4 C–Br vibrations

Most aromatic bromo compounds absorb strongly in the region  $650\text{--}395\text{ cm}^{-1}$  due to C–Br stretching vibrations, although there are more than one bromine atoms on the same carbon atom. The C–Br stretching vibration is assigned to the weak mode  $656\text{ cm}^{-1}$  in the infrared spectra. The in-plane C–Br bending mode is observed at  $548\text{ cm}^{-1}$ , while the out-of-plane bending mode is at  $152\text{ cm}^{-1}$  in Raman spectrum.

#### 6.4.5 Methyl group vibrations

BMB under consideration possesses a  $\text{CH}_3$  group in the side-substituted chain. For the assignments of  $\text{CH}_3$  group frequencies, one can expect that nine fundamentals can be associated with each  $\text{CH}_3$  group, namely the symmetrical stretching in  $\text{CH}_3$  ( $\text{CH}_3$  symmetric stretch) and asymmetrical stretching ( $\text{CH}_3$  asymmetric stretch) in-plane stretching modes (i.e., in-plane hydrogen stretching mode); the symmetrical ( $\text{CH}_3$  symmetric deform) and asymmetrical ( $\text{CH}_3$  asymmetric deform) deformation modes; the in-plane rocking ( $\text{CH}_3$  ipr), out-of-plane rocking ( $\text{CH}_3$  opr), and twisting ( $\text{tCH}_3$ ) modes. Methyl groups are generally referred as electron-donating substituents in the aromatic ring system. The methyl hydrogen atoms in BMB are subjected simultaneously to hyperconjugation and backdonation, which causes the decrease in stretching wavenumbers and infrared intensities, as reported in literature [32], for similar molecular system. For the O– $\text{CH}_3$  group compounds [33], the asymmetric stretching mode appears in the range  $2825\text{--}2870\text{ cm}^{-1}$ , lower in magnitude compared with the value in  $\text{CH}_3$  compounds ( $2860\text{--}2935\text{ cm}^{-1}$ ), whereas the asymmetric stretching modes for both types of compounds lie in the same region, 2924 and  $2985\text{ cm}^{-1}$ . In case of BMB, asymmetric and symmetric stretching vibrations of  $\text{CH}_3$  group have been identified at 2970, 2968, and  $2930\text{ cm}^{-1}$  by B3LYP/6-311++G (d, p) method. The recorded FT-IR spectrum show two weak bands observed at 2976, 2964, and  $2928\text{ cm}^{-1}$ , which are assigned to C–H asymmetric and symmetric vibrations of a  $\text{CH}_3$  group for BMB. The rocking vibrations for  $\text{CH}_3$  group have been calculated at 1015 and  $894\text{ cm}^{-1}$  by B3LYP/6-311++G (d, p) method, which also shows good agreement with FT-IR and FT-Raman recorded values at 1012 and  $895\text{ cm}^{-1}$  for BMB, respectively.

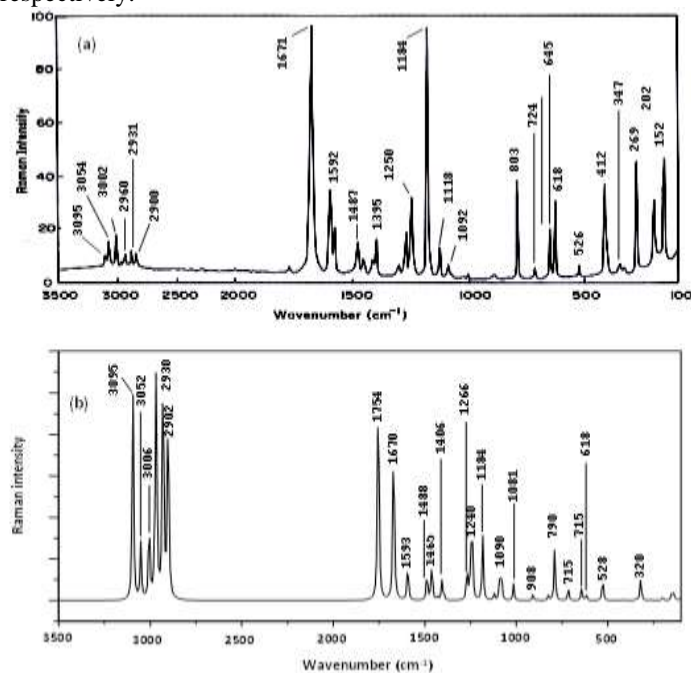


**Fig. 7.** FT Raman spectrum of 5-bromo-2-methoxybenzaldehyde (a) Observed (b) Calculated by B3LYP/6-311++G (d, p)

The asymmetrical  $\text{CH}_3$  deformation vibrations are computed by B3LYP++G (d, p) method at  $1593\text{ cm}^{-1}$ . Similarly, the symmetrical deformation vibration of  $\text{CH}_3$  group is computed at  $1465\text{ cm}^{-1}$  for BMB. These fundamental values show good agreement with the observed FT-IR and FT-Raman values 1592

and  $1465\text{ cm}^{-1}$ . These assignments find support from the work of Varsanyi [34].

#### 6.4.6. O-CH<sub>3</sub> vibrations

The O-CH<sub>3</sub> mode is assigned to  $\sim 1040\text{ cm}^{-1}$  for anisole [35] and to the region  $1000\text{--}1100\text{ cm}^{-1}$  for anisole and its derivatives [37–38]. This mode is assigned to 1026, 909 and  $995\text{ cm}^{-1}$  for *o*-, *m*- and *p*-methoxybenzaldehyde, respectively. In our case the O-CH<sub>3</sub> stretching mode is assigned as strong bands in FT-IR at  $1250$  and  $1084\text{ cm}^{-1}$ . The theoretically computed values at  $1245$  and  $1081\text{ cm}^{-1}$  using B3LYP/6-311++G (d, p) method coincide with experimental results.

The C-O-CH<sub>3</sub> bending mode is assigned near  $300\text{ cm}^{-1}$  for anisole by Owen and Hester [37] and at  $421\text{ cm}^{-1}$  for *p*-methoxybenzaldehyde by Compagnaro and Wood [38]. Ramana Rao and co-workers [36] have proposed assignment for this mode in the region  $300\text{--}670\text{ cm}^{-1}$  for anisole and its derivatives. As this mode lies in the region of the ring planar C-C-C angle bending modes, a strong mixing among these two modes and other planar modes is expected. Krishnakumar *et.al.* [39] assigned C-O-CH<sub>3</sub> angle bending mode at 341, 382 and  $430\text{ cm}^{-1}$  for the *o*-, *m*- and *p*-methoxybenzaldehydes, respectively. In accordance with above we have assigned the theoretically computed values by B3LYP/6-311++G (d, p) method at  $643$  and  $634\text{ cm}^{-1}$  for BMB as C-O-CH<sub>3</sub> angle bending mode, the value that coincides with  $645$  and  $632\text{ cm}^{-1}$  bands observed in FT-Raman.

The torsion mode of the O-CH<sub>3</sub> group was observed for anisole at  $100\text{ cm}^{-1}$  by some workers [22]. The computed values predicted by B3LYP/6-311++G (d, p) method at 265 and  $200\text{ cm}^{-1}$  correlate with experimental observation for O-CH<sub>3</sub> torsion mode for BMB.

#### 7. NBO analysis

The first two columns in the Table 8 show the type of orbital and occupancy between 0 and 2.000 electrons. The type can be bonding, lone pair and antibonding. A normal Lewis structure would not have any antibonding orbital, so the presence of antibonding orbitals leads to deviation from normal Lewis structure. Antibonding localized orbital is called non-Lewis NBO. If the occupancy is not 2.000, then there is deviation from an ideal Lewis structure. The BMB molecule shows some deviations; otherwise it is well approximated using Lewis structure.

In Table 10, BD (O10-C11) orbital with 1.99331 electrons has 68.19% O10 character in a  $sp^{2.67}$  hybrid and has 31.81% C11 character in a  $sp^{23.69}$  hybrid. The  $sp^{2.10}$  hybrid on O10 has 72.73% *p*-character and the  $sp^{2.66}$  hybrid on C has 78.46% *p*-character. An idealized  $sp^2$  hybrid has 75% *p*-character. The BD (O10-C11) bond then corresponds roughly to the quantitative concept of interacting  $sp^3$  hybrids. The two coefficients, 0.8258 and 0.5640, are called polarization coefficients. The sizes of these coefficients show the importance of the two hybrids in the formation of the bond. The oxygen has larger percentage of this NBO, 68.19% and gives the larger polarization coefficient 0.8258 because it has the higher electronegativity. Similarly, BD (C2-O10), BD (C4-C5), BD (C5-Br17), BD (C7-O8), BD (C1-C2), and bonding orbital also show that nitrogen and chlorine have the lesser percentage of NBO and give the lesser polarization coefficients as compared to BD (O10-C11) bond. This shows that oxygen and bromine in above bonding orbital have less electronegativity as compared to BD (O10-C11). At

the end of the table, nitrogen and chlorine lone pair NBO is expected to attain the Lewis structure.

#### 7.1 Perturbation theory analysis

Delocalization of the electron density between occupied Lewis type (bond (or) lone pair) NBO orbital and formally unoccupied (antibond or Rydberg) non-Lewis NBO orbital corresponds to a stabilized donor-acceptor interaction. The energy of this interaction can be estimated by the second-order perturbation theory [15]. Table 9 lists the calculated second order interaction energies  $E^{(2)}$  between the donor-acceptor orbital of BMB.

The most important interaction energies related to the resonance in the benzene ring are electron donating from the BD (C1-C2), BD (C1-C6), BD (C6-H18), and LPO10, to the antibonding acceptor BD\* (C1-C6), BD\* (C1-C2), BD\* (C1-C2), and BD\* (C2-C3), orbitals and their corresponding energies, are 3.69, 4.07, 4.20, and 4.58 kcal/mol, respectively. These interactions clearly indicate that the strongest increase in the stabilization energy of electron delocalization occurs due to the substitution of the molecule.

#### 8. HOMO-LUMO band gap

The conjugated molecules are characterized by the separation between highest occupied molecular orbital and lowest unoccupied molecular orbital (HOMO-LUMO), which is the result of a significant degree of intramolecular charge transfer (ICT) from the end-capping electron-donor groups through  $\pi$ -conjugated path. The strong charge transfer interaction through  $\pi$ -conjugated bridge results in substantial ground state donor-acceptor mixing and the appearance of a charge transfer band in the electronic absorption spectrum of a charge transfer band in the electronic absorption spectrum. Therefore, an ED transfer occurs from the more aromatic part of the  $\pi$ -conjugated system in the electron-donor side to its electron-withdrawing part the atomic orbital components of the frontier molecular orbitals are shown in Fig. 8.

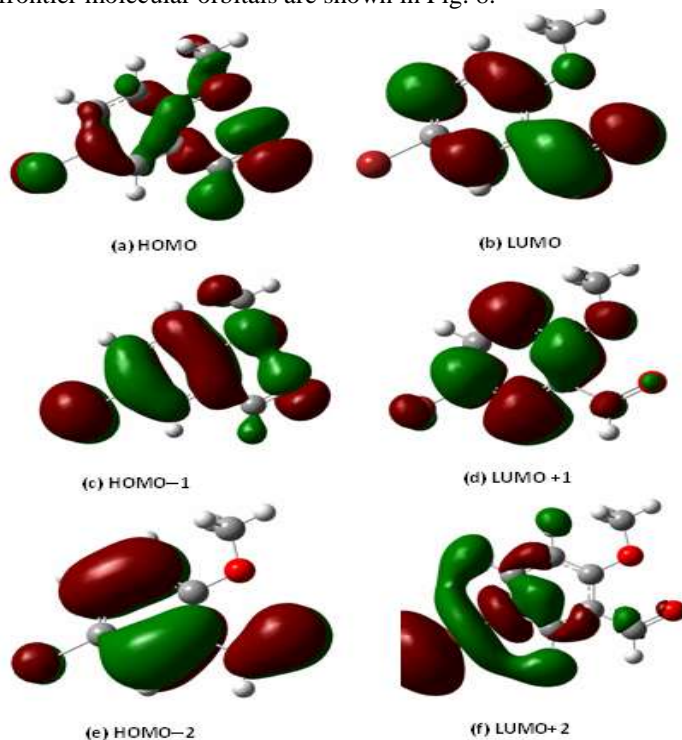


Fig. 8. HOMO-LUMO picture of 5-bromo-2-methoxybenzaldehyde

**Table 1.** The electric dipole moment  $\mu$  (Debye), the mean polarizability  $\alpha$  ( $\times 10^{-22}$  esu), anisotropy polarizability  $\Delta\alpha$  ( $\times 10^{-25}$  esu) and first hyperpolarizability  $\beta_{\text{tot}}$  ( $\times 10^{-31}$  esu) for 5-bromo-2-methoxybenzaldehyde

Parameters	Values	Parameters	Values
$\mu_x$	2.7078	$\beta_{xxx}$	-26.1792
$\mu_y$	-5.5051	$\beta_{yyy}$	-64.5115
$\mu_z$	0.0002	$\beta_{zzz}$	-0.0025
$\mu$	5.6975	$\beta_{xyy}$	-28.0732
$\alpha_{xx}$	-67.9730	$\beta_{xxy}$	-24.5994
$\alpha_{xy}$	-10.0445	$\beta_{xxz}$	0.0103
$\alpha_{xz}$	-0.0019	$\beta_{xzz}$	-22.3474
$\alpha_{yy}$	-81.8325	$\beta_{yzz}$	2.7657
$\alpha_{yz}$	0.0010	$\beta_{yyz}$	-0.0023
$\alpha_{zz}$	-78.5764	$\beta_{xyz}$	-0.0035
$\alpha$	0.0000	$\beta_{\text{tot}}$	11.5
$\Delta\alpha$	19.2950		

**Table 2.** Calculated energies and energy difference for four conformers of 5-bromo-2-methoxybenzaldehyde by DFT method

Conformers	B3LYP/6-311++G (d)		B3LYP/6-311++G (d, p)	
	Energy (kJ/mol)	Energy differences <sup>a</sup> (kJ/mol)	Energy (kJ/mol)	Energy differences <sup>a</sup> (kJ/mol)
C1	-7965090.49	0.000	-7965150.08	0.000
C2	-7964895.67	194.82	-7965138.53	11.50
C3	-7964831.35	259.14	-7965121.20	28.88
C4	-7963917.41	1173.08	-7965117.53	32.54

<sup>a</sup>Energies of the other three conformers relative to the most stable C1 conformer.**Table 3.** Optimized geometrical parameters of 5-bromo-2-methoxybenzaldehyde by B3LYP/6-311++G (d) /6-311++G (d, p) calculations.

Parameters	Bond lengths (Å)			Parameters	Bond angles (°)		
	Exp <sup>a</sup>	6-311++G (d)	6-311++G (d, p)		Exp <sup>a</sup>	6-311++G (d)	6-311++G (d, p)
C1-C2	1.42	1.40	1.41	C2-C1-C6	119.9	118.7	119.6
C1-C6	1.38	1.39	1.39	C2-C1-C7	120.0	120.6	121.4
C1-C7	1.42	1.47	1.48	C6-C1-C7	120.0	120.6	118.9
C2-C3	1.42	1.37	1.39	C1-C2-C3	120.0	120.1	119.4
C3-C4	1.42	1.41	1.39	C1-C2-O10	116.7	120.1	116.7
C3-H15	1.10	1.08	1.08	C3-C2-O10	120.8	119.7	123.8
C4-C5	1.41	1.41	1.39	C2-C3-C4	120.1	122.0	120.1
C4-O10	1.10	1.08	1.08	C2-C3-H15	120.1	121.3	120.9
C5-C6	1.38	1.39	1.38	C4-C3-H15	119.3	116.6	118.8
C6-H18	1.09	1.08	1.08	C3-C4-C5	120.0	117.5	120.0
C7-O8	1.20	1.21	1.21	C3-C4-O10	120.1	112.0	119.6
C7-H9	1.11	1.11	1.10	C5-C4-O10	120.2	130.4	120.2
O10-C11	1.40	1.43	1.42	C5-C6-H18	119.9	119.8	121.7
C11-H12	1.09	1.08	1.08	C1-C7-O8	122.7	125.3	123.5
C11-H13	1.09	1.08	1.09	C1-C7-H9	118.2	114.5	115.6
C11-H14	1.09	1.08	1.09	O8-C7-H9	120.0	120.1	120.8
C4-H16	1.10	1.08	1.09	C2-O10-C11	120.1	126.7	119.2
C2-O10		1.35	1.09	O10-C11-H12	109.2	104.1	105.6
C5-Br17		1.92	1.35	O10-C11-H13	109.7	111.5	111.2
				O10-C11-H14	110.1	111.5	111.2
				C11-H12-H14	109.5	109.5	109.4
				C11-H12-H13	109.6	109.5	109.8
				C4-C5-C6		20.1	120.4
				C4-C5-Br17		125.0	119.5
				C6-C5-Br17		114.8	120.0
				C1-C6-C5		121.5	120.2
				C1-C6-H18		118.5	117.9

<sup>a</sup>Geometrical parameters determined with X-ray diffraction method taken from Ref. [7].

**Table 6. Vibrational wavenumbers(unscaled and scaled) obtained for C1 conformer of BMB at DFT/ B3LYP/6-311++G (d) and 6-311++G (d, p) [harmonic frequency (cm<sup>-1</sup>), IR intensities (Kcal mol<sup>-1</sup>), Raman activities (Å amu<sup>-1</sup>),**

S. No.	Unscaled		Scaled		IR intensity		Raman activity	
	A	B	A	B	A	B	A	B
1	3204	3213	3099	3095	2.30	4.83	48.24	133.35
2	3196	3203	3058	3052	4.70	3.90	147.70	34.34
3	3167	3195	3010	3006	7.59	1.09	72.70	53.07
4	3147	3140	2978	2970	22.0	15.19	120.10	117.27
5	3144	3078	2976	2968	18.20	29.62	36.68	59.61
6	3089	3014	2940	2930	52.30	50.99	166.91	173.73
7	3044	2981	2908	2902	143.90	65.37	201.70	139.56
8	1793	1799	1758	1754	317.89	290.51	186.50	119.21
9	1730	1722	1696	1687	223.91	71.23	256.70	86.61
10	1712	1708	1679	1670	2.78	12.30	7.08	17.91
11	1620	1622	1598	1593	107.40	64.68	0.89	12.78
12	1563	1560	1484	1488	12.25	128.23	14.90	4.48
13	1548	1544	1464	1465	17.64	10.44	7.48	13.64
14	1511	1507	1452	1460	26.29	28.74	5.89	1.77
15	1482	1470	1426	1430	4.26	27.76	0.73	8.62
16	1440	1451	1410	1404	16.70	98.56	12.28	2.16
17	1420	1425	1399	1395	349.12	22.74	51.58	5.23
18	1307	1310	1280	1272	6.30	181.20	0.93	7.84
19	1293	1290	1272	1266	135.40	130.10	3.73	20.06
20	1288	1281	1253	1245	83.45	35.50	17.66	20.56
21	1260	1261	1244	1240	128.60	54.68	35.57	26.63
22	1204	1210	1188	1184	0.74	0.73	2.61	2.55
23	1187	1180	1115	1116	25.94	71.14	3.35	8.33
24	1120	1122	1098	1090	8.25	1.47	1.29	10.65
25	1110	1112	1080	1081	59.97	48.31	7.75	6.36
26	1060	1052	1016	1015	2.34	0.80	3.45	2.51
27	979	970	906	908	1.18	1.19	0.04	0.04
28	938	931	897	894	10.81	9.16	0.55	0.24
29	912	911	880	883	33.70	29.77	10.41	1.84
30	863	860	831	825	40.88	35.19	0.17	0.18
31	850	849	816	810	15.60	7.38	6.69	18.97
32	833	829	810	804	0.41	0.00	0.23	0.71
33	827	820	794	790	15.05	13.86	9.99	3.61
34	750	751	729	720	44.65	29.03	1.28	4.29
35	741	735	725	715	3.55	6.52	0.16	0.16
36	681	680	660	656	11.09	32.78	4.46	2.20
37	670	666	651	643	3.45	2.98	0.01	0.03
38	651	650	636	634	3.00	1.32	15.30	8.45
39	640	639	622	618	2.69	0.23	1.00	0.38
40	566	563	545	549	3.07	2.98	2.92	0.63
41	533	531	526	528	2.66	2.67	2.71	8.02
42	427	425	415	410	0.05	0.75	0.89	0.30
43	360	354	346	345	0.72	0.17	1.02	1.36
44	341	340	320	320	4.80	5.04	2.08	2.86
45	280	281	270	265	0.64	2.86	1.83	1.93
46	213	209	203	200	4.42	12.44	2.50	0.59
47	162	160	154	151	7.01	0.23	1.72	0.73
48	84	82	68	65	5.17	0.72	0.08	0.54

**Table 10. Selected HOMO and LUMO energies of 5-bromo-2-methoxybenzaldehyde.**

S No	Molecular orbital	Energy	eV	Molecular orbital Energy transitions	Energy gap eV
1	HOMO	-6.664		HOMO→LUMO	-2.76
2	HOMO-1	-6.691		HOMO-1→LUMO	-2.787
3	HOMO-2	-7.741		HOMO-2→LUMO	-3.837
4	LUMO	-3.904		HOMO→LUMO+1	-4.298
5	LUMO+1	-2.366		HOMO-1→LUMO+1	-4.325
6	LUMO+2	-2.022		HOMO-2→LUMO+1	-5.719
				HOMO→LUMO+2	-4.642
				HOMO-1→LUMO+2	-4.669
				HOMO-2→LUMO+2	-5.719

**Table 11. Experimental and theoretical chemical shifts of BMB in <sup>1</sup>H and <sup>13</sup>C NMR spectra [δ (ppm)]**

Atom position	Experimental	Calculated B3LYP/6-311++G (d, p)	Δ
C1	126.05	130.43	4.38
C2	138.23	129.84	-8.39
C3	113.82	109.78	-4.04
C4	160.73	161.31	0.58
C5	113.37	121.79	8.42
C6	130.80	132.58	1.78
C7	188.16	198.12	9.96
C12	55.98	44.40	-11.58
H10	10.38	10.60	0.32
H13	3.92	2.25	0.67
H16	6.69	6.89	0.20
H17	7.04	7.62	0.58
H19	7.91	8.14	0.23

Δ (δ<sub>exp</sub>-δ<sub>the</sub>): difference between respective chemical shifts.

**Table 7. Experimental FTIR and FT Raman frequencies( $\text{cm}^{-1}$ ) and assignments for C1 conformer of BMB**

Mode	Species	FTIR <sup>a</sup>	FT-Raman <sup>a</sup>	Vibrational assignments <sup>b</sup> (%PED)
1	A'	3098w	3095w	vCH (99)
2	A'	3048w	3054w	vCH (99)
3	A'	2998w	3002w	vCH (98)
4	A''	2976w		v <sub>as</sub> CH <sub>3</sub> (99)
5	A'	2964ms	2960w	v <sub>as</sub> CH <sub>3</sub> (84)
6	A'	2928w	2931w	v <sub>ss</sub> CH <sub>3</sub> (80)
7	A'	2898w	2900w	vCH (99)
8	A'	1758vs		vCO (69)
9	A'	1690vs		vCC (62)
10	A'		1671vw	vCC (73)
11	A''		1592ms	CH <sub>3</sub> asd (68)
12	A'		1487w	bCH (47)
13	A'	1468vs	1465vw	CH <sub>3</sub> sd(69)
14	A'	1456vs		bCH (52)
15	A'	1432vs		vCC (69)
16	A'		1408vw	CH <sub>3</sub> sd (55)
17	A'	1396vs	1395w	bCH (77)
18	A'		1276ms	vCC (73)
19	A'	1264vs		vCC (69)
20	A'		1250ms	vCO (68)
21	A''	1239s		gCH (65)
22	A''	1181vs	1184vs	gCH (62)
23	A'	1120s	1118w	vCC (75)
24	A'		1092w	vCC (92)
25	A'	1084w		vCO (69)
26	A'	1012vs		CH <sub>3</sub> ipr (68)
27	A''	908vw		gCH (60)
28	A''		895vw	CH <sub>3</sub> opr (60)
29	A''	884ms		gCH (65)
30	A'	824s		bring (70)
31	A'	812vw		bring (68)
32	A'		803ms	bCO (70)
33	A'	788w		bring (70)
34	A''		724vw	gCH (60)
35	A'	716vw		bCC (55)
36	A'	656ms		vCBr (54)
37	A'		645ms	bCO(50)
38	A'	632ms		bCO (48)
39	A''		618ms	gring (61)
40	A'	548vw		bCBr (48)
41	A''	524ms	526vw	gring (60)
42	A''		412ms	gCC (50)
43	A''		347vw	gring (58)
44	A''		321vw	gCO (45)
45	A''		269ms	gCO (48)
46	A''		202ms	gCO (45)
47	A''		152ms	gCBr (42)
48	A''			CH <sub>3</sub> torsion(41)

<sup>a</sup> Intensities: w-weak, vw-very weak, m-medium, s-strong, vs-very strong.

<sup>b</sup> Assignments: v-stretching, b-inplane bending, g- out-of- plane bending.

**Table 8. NBO results showing the formation of Lewis and non Lewis orbital the valence hybrids corresponding to the intramolecular CH<sub>3</sub> .....Br Hydrogen bonds in BMB.**

BOND(A-B)	ED/ ENERGY (a.u)	ED <sub>A</sub> (%)	ED <sub>B</sub> (%)	NBO	S(%)	P(%)
BD(1)C1-C7	1.97911	53.38	46.62	0.7306(sp <sup>2.50</sup> ) <sub>C+</sub> 0.6828(sp <sup>1.83</sup> ) <sub>C</sub>	28.59 35.32	71.37 64.64
BD(1)C4-O10	1.98861	32.86	67.14	0.5732(sp <sup>3.27</sup> ) <sub>C+</sub> 0.8194(sp <sup>2.59</sup> ) <sub>O</sub>	23.38 27.87	76.40 72.06
BD(1)C3-H15	1.97388	61.06	38.94	0.7814(sp <sup>2.36</sup> ) <sub>C+</sub> 0.6240(sp <sup>0.00</sup> ) <sub>H</sub>	29.72 99.95	70.24 0.05
BD(1)C2-O10	1.97899	61.08	38.92	0.7815(sp <sup>2.45</sup> ) <sub>C+</sub> 6239(sp <sup>0.00</sup> ) <sub>H</sub>	28.95 99.95	71.01 0.05
BD(1)C5-Br17	1.98491	49.97	50.03	0.7069(sp <sup>3.42</sup> ) <sub>C+</sub> 0.7073(sp <sup>6.40</sup> ) <sub>Br</sub>	22.61 13.46	77.26 86.14
BD(1)C7-O8	1.99637	35.21	64.79	0.5934(sp <sup>2.26</sup> ) <sub>C+</sub> 0.8049(sp <sup>1.80</sup> ) <sub>O</sub>	30.64 35.65	69.15 64.24
BD(1)C7-H9	1.98931	58.46	41.54	0.7646(sp <sup>1.97</sup> ) <sub>C+</sub> 0.6445(sp <sup>0.00</sup> ) <sub>H</sub>	33.61 99.94	66.31 0.06
BD(1)O10-C11	1.99331	68.19	31.81	0.8258(sp <sup>2.67</sup> ) <sub>O+</sub> 0.5640(sp <sup>3.69</sup> ) <sub>C</sub>	27.20 21.25	72.73 78.46
BD* (1)C1-C7	0.06012	46.62	53.38	0.6828(sp <sup>2.50</sup> ) <sub>C+</sub> -0.7306(sp <sup>1.83</sup> ) <sub>C</sub>	28.59 35.32	71.37 64.64
BD* (1)C4-H16	0.03294	67.14	32.86	0.8194(sp <sup>3.27</sup> ) <sub>C+</sub> -0.5732(sp <sup>2.59</sup> ) <sub>O</sub>	23.38 27.87	76.40 72.06
BD* (1)C3-H15	0.01488	38.94	61.06	0.6240(sp <sup>2.36</sup> ) <sub>C+</sub> -0.7814(sp <sup>0.00</sup> ) <sub>H</sub>	29.72 99.95	70.24 0.00
BD* (1)C4-C5	0.02633	50.11	48.89	0.7079(sp <sup>1.82</sup> ) <sub>C+</sub> -0.7063(sp <sup>1.58</sup> ) <sub>C</sub>	35.45 38.72	64.50 61.23
BD* (1)C2-O10	0.01364	38.92	61.08	0.6239(sp <sup>2.45</sup> ) <sub>C+</sub> -0.7815(sp <sup>0.00</sup> ) <sub>H</sub>	28.95 99.95	71.01 0.00
BD* (1)C5-Br17	0.03317	50.03	49.97	0.7073(sp <sup>3.42</sup> ) <sub>C+</sub> -0.7069(sp <sup>6.40</sup> ) <sub>Br17</sub>	22.61 13.46	77.26 86.14
BD* (1)C6-H18	0.01415	37.93	62.07	0.6159(sp <sup>2.40</sup> ) <sub>C+</sub> -0.7878(sp <sup>0.00</sup> ) <sub>H</sub>	29.40 99.99	70.51 0.00
BD* (1)C7-O8	0.00237	64.79	35.21	0.8049(sp <sup>2.06</sup> ) <sub>C+</sub> -0.5934(sp <sup>1.80</sup> ) <sub>O</sub>	30.64 35.65	69.15 64.24
BD* (1)C7-H9	0.04378	41.54	58.46	0.6445(sp <sup>1.97</sup> ) <sub>C+</sub> -0.7646(sp <sup>0.00</sup> ) <sub>H</sub>	33.61 99.94	66.31 0.00
BD* (1)O10-C11	0.00562	31.81	68.19	0.5640(sp <sup>2.67</sup> ) <sub>O+</sub> -0.8248(sp <sup>3.69</sup> ) <sub>C</sub>	27.20 21.25	72.73 78.46
BD* (1)C11-H12	0.00972	40.19	59.81	0.6340(sp <sup>2.78</sup> ) <sub>C+</sub> -0.7734(sp <sup>0.00</sup> ) <sub>H</sub>	26.43 99.96	73.51 0.00
BD* (1)C11-H13	0.01711	41.19	58.81	0.6418(sp <sup>2.81</sup> ) <sub>C+</sub> -0.7669(sp <sup>0.00</sup> ) <sub>H</sub>	26.24 99.96	73.69 0.00
LP (1) O8	1.98719	---	---	sp <sup>0.57</sup>	63.65	36.64
LP (1) O10	1.97102	---	---	sp <sup>1.22</sup>	45.01	54.97
LP (1) Br17	1.99345	---	---	sp <sup>0.15</sup>	86.76	13.24

**Table 9. The second order perturbation energies E<sup>(2)</sup> (kcal/mol) corresponding to the most important charge transfer interactions (donor-acceptor) in the compounds studied by B3LYP/ 6-311++G (d, p) method for BMB.**

Donor NBO (i)	Acceptor NBO (j)	E <sup>(2)</sup> (kcal/mol)	E(j)-E(i)(a.u)	F(i,j)(a.u)
BD(1)C1-C2	BD*(1)C1-C6	3.69	1.29	0.062
BD(1)C1-C2	BD*(1)C1-C7	1.08	1.10	0.031
BD(1)C1-C2	BD*(1)C2-C3	4.05	1.28	0.064
BD(1)C1-C2	BD*(1)C3-H15	2.17	1.18	0.045
BD(1)C1-C2	BD*(1)C6-H18	1.98	1.19	0.043
BD(1)C1-C2	BD*(1)C7-O8	0.65	1.24	0.025
BD(1)C1-C2	BD*(1)O10-C11	1.65	1.00	0.036
BD(1)C1-C6	BD*(1)C1-C2	4.07	1.28	0.064
BD(1)C1-C6	BD*(1)C1-C7	1.28	1.08	0.033
BD(1)C1-C6	BD*(1)C2-O10	4.21	0.98	0.057
BD(1)C1-C6	BD*(1)C5-C6	3.67	1.27	0.067
BD(1)C1-C6	BD*(1)C5-Br17	5.12	0.81	0.057
BD(1)C1-C6	BD*(1)C6-H18	1.15	1.17	0.033
BD(1)C1-C7	BD*(1)C7-H9	0.69	1.13	0.025
BD(1)C1-C7	BD*(1)C1-C2	1.33	1.20	0.036
BD(1)C1-C7	BD*(1)C1-C6	1.49	1.20	0.038
BD(1)C1-C7	BD*(1)C2-C3	3.26	1.18	0.056
BD(1)C1-C7	BD*(1)C2-O10	0.53	0.91	0.020
BD(1)C2-C3	BD*(1)C1-C2	4.54	1.29	0.068
BD(1)C2-C3	BD*(1)C1-C7	3.16	1.09	0.053
BD(1)C2-C3	BD*(1)C3-H15	1.33	1.17	0.035
BD(1)C2-O10	BD*(1)C1-C6	1.72	1.40	0.044
BD(1)C2-O10	BD*(1)C3-C4	1.36	1.40	0.039
BD(1)C2-O10	BD*(1)C11-H14	0.80	1.25	0.028
BD(1)C3-C4	BD*(1)C2-C3	3.18	1.26	0.057
BD(1)C3-C4	BD*(1)C2-O10	4.14	0.98	0.057
BD(1)C3-C4	BD*(1)C3-H15	1.50	1.16	0.037
BD(1)C3-C4	BD*(1)C4-C5	3.76	1.27	0.062
BD(1)C3-C4	BD*(1)C4-H16	1.03	1.16	0.031
BD(1)C3-C4	BD*(1)C5-Br17	5.27	0.81	0.058
BD(1)C3-H15	BD*(1)C1-C2	3.93	1.11	0.059
LP(1) O8	BD*(1)C1-C7	0.07	1.09	0.026
LP(1) O8	BD*(1)C7-H9	0.55	1.14	0.022
LP(1) O12	BD*(1)C2-C3	4.58	1.15	0.065
LP(1) O12	BD*(1)C11-H14	2.15	1.02	0.042
LP(1) Br17	BD*(1)C4-C5	1.67	1.54	0.046
LP(1) Br17	BD*(1)C5-C6	1.57	1.54	0.044

The Fig. 8 shows molecular orbitals from HOMO-2 to LUMO+2 of BMB, in which all the LUMO surfaces are well localized within the phenyl ring. In other words all the ring component intermolecular interactions are mostly occurred in LUMO levels. LUMO+1 and LUMO+2 surfaces shown in Figs. 8d, 8f, have no amplitude [22] on aldehyde group linked to six member ring of BMB. In HOMO-2, the orbitals are well localized on aldehyde group of BMB. In HOMO-2, H9 in aldehyde group is highly coupled with C7 and C1. Moreover,  $H_9^+$  and  $O_8^-$  interaction is also present in this orbital. Most of the surfaces shown in the HOMO side have no amplitude on phenyl ring but, all the HOMO surfaces (Figs. 8a, 8c, and 8e) have very high amplitude on aldehyde group of BMB.

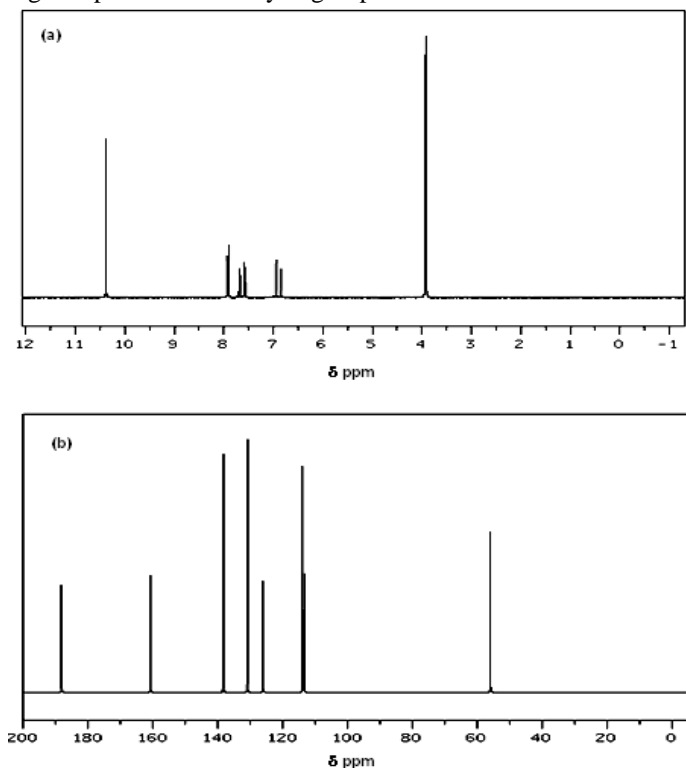


Fig. 9. NMR spectra of 5-bromo-2-methoxybenzaldehyde. (a)  $^1\text{H}$  (b)  $^{13}\text{C}$

The presence of intramolecular charge transfer from donor to acceptor group within molecule can be identified by analyzing the co-existence of IR and Raman activity [23] itself. It is also observed that in our BMB that the bands at 3098, 1468, 1181, 1120 and 524  $\text{cm}^{-1}$  in FT-IR spectrum have their counterparts in FT-Raman at 3095, 1465, 1184, 1118 and 526  $\text{cm}^{-1}$ , which shows that the relative intensities in IR and Raman are comparable resulting from the electron cloud movement through single-double bond  $\pi$ -conjugated path from donor to acceptor groups. The analysis of wave function indicates that the electron absorption corresponds to the transition from the ground state to the first excited state and is mainly described by one-electron excitation from the HOMO to LUMO. The HOMO and LUMO energies of BMB have been calculated at B3LYP/6-31G (d, p) level which is presented in Table 10. The energy gap presented in Table 10 reflects the chemical activity of the molecule. HOMO represents the ability to donate an electron and LUMO represents the ability to accept an electron. Among the six subsequent excited states calculated, the strongest transitions appear between HOMO-LUMO orbitals. The numerical value of energy gap between HOMO-LUMO orbitals calculated at

B3LYP level is -2.76 eV. The energy gaps for other possible energy transitions are presented in Table 10.

### 9. $^1\text{H}$ and $^{13}\text{C}$ NMR spectral analyses

The molecular structure of BMB is optimized by using B3LYP method with 6-311++G (d, p). Then, gauge invariant atomic orbital (GIAO)  $^1\text{H}$  and  $^{13}\text{C}$  calculations of BMB are calculated and compared with experimental data which are shown in Table 11. The  $^1\text{H}$  and  $^{13}\text{C}$  NMR spectra are presented in Fig. 9. The result shows that the range of  $^1\text{H}$  and  $^{13}\text{C}$  NMR chemical shift of the typical organic molecule is usually > 100 ppm [40, 41] the accuracy ensures reliable interpretation of spectroscopic parameters. It is true from the above literature value in our present study; BMB also shows the same. The molecular structure of BMB shows that the bromine atom presents at 5th position of the ring carbon. This bromine atom shows electronegative property (they attract the other atom towards), but the chemical shift of C5 seems to be (C5 = 121.79) by B3LYP/6-311++G (3d,3p) method which is same for other carbon atoms but in C7 the chemical shift has higher value i.e. 198.12 ppm using B3LYP/6-311++G (3d,3p) method. On the other hand the isotropic chemical shifts for the other carbon and hydrogen atoms are shown in Table 11.

### 10. Conclusion

We have carried out density functional theory calculations on the structure, vibrational spectrum, hyperpolarizability, NBO, HOMO-LUMO analyses and  $^1\text{H}$  and  $^{13}\text{C}$  NMR of BMB. The equilibrium geometry by B3LYP/6-311++G (d, p) level for both the bond lengths and bond angles is performed better. The vibration frequency analysis by B3LYP/6-311++G (d, p) method agrees satisfactorily with experimental results. On the basis of agreement between the calculated and experimental results, assignments of all the fundamental vibrational modes of BMB are examined and proposed in this investigation. Therefore, the assignments made at higher level of theory with higher basis set with only reasonable deviations from the experimental values, seems to be correct. Based on calculated energy differences, the C1 conformer is found to be the most stable conformer. Intermolecular hydrogen bonding between H and O is expected in C1 conformer. The electric dipole moments and first hyperpolarizability of the compound studied have been calculated by DFT method with 6-311++G (d, p) basis set. The DFT calculated non-zero  $\mu$  value of this ligand shows that the BMB compound might have microscopic first hyperpolarizability with non-zero values obtained by the numerical second derivatives of the electric dipole moment according to the applied field strength. The high degree of stabilization emanating from strong mesomeric effects has been well demonstrated by NBO analysis. The second-order perturbation theory results show that the  $\text{CH}_3$  group behaves as separate unit with sufficient interaction energy. The lowering of HOMO-LUMO band gap supports bioactive property of the molecule.  $^1\text{H}$  and  $^{13}\text{C}$  NMR isotropic chemical shifts were calculated and the assignments made are compared with the experimental values.

### References

- [1] <http://w.w.chemicaland21.com/>
- [2] S.K. Vaish, A.K. Anupam Singh, N.K. Singh, Malhotra, Indian J. Pure Appl. Phys. 43 (2005) 295-300.
- [3] T. Narayan Akinchan, R. Akinchan, Indian J. Chem. 41A (2002) 1152-1156.
- [4] T. Imai, M. Maekawa, S. Tsuchiya, Appl. Entomol. Zool. 37 (2002) 505-508.

- [5] S. Mohan, S. Gunasekaran, S. Kalainathan, *Acta Ciencia India* XIV (1988) 77–84.
- [6] V. Ramana Rao, Ph.d., Thesis, Kakatiya University, (1998).
- [7] S. Gunasekaran, S. Seshadri, S. Muthu, *Asian J. Chem.* 19 (2007) 465–471.
- [8] N.C. Handy, C.W. Murray, R.D. Amos, *J. Phys. Chem.* 97 (1993) 4392–4396.
- [9] P.J. Stephans, F.J. Devlin, C.F. Chavalowski, M.J. Frisch, *J. Phys. Chem.* 99 (1995) 16883–16902.
- [10] A. Frisch, A.B. Niesen, A.J. Holder, *GaussView user Manual*, Gaussian Inc., (2008).
- [11] M.J. Frisch, G.W. Trucks, H.B. Schlegel, G.E. Scuseria, M.A. Robb, et al. *Gaussian 09*, Revision A. 02, Gaussian, inc, Wallingford CT, (2009).
- [12] A.D. Becke, *J. Chem. Phys.* 98 (1993) 785–789.
- [13] C. Lee, W. Yang, R.G. Parr, *Phys. Rev. B* 37 (1993) 5648–5652.
- [14] P.L. Polavarapu, *J. Phys. Chem.* 94 (1990) 8106–8112.
- [15] A. E. Reed, F. Weinhold, *J. Chem. Phys.* 78 (1983) 4066–4073.
- [16] J. Chocholousova, V. Vladimir Spirko, P. Hobza, *Phys. Chem. Chem. Phys.* 6 (2004) 37–41.
- [17] C.R. Zhang, H.S. Chen, G.H. Wang, *Chem. Res. Chinese U* 20 (2004) 640–643.
- [18] C. James, A. Amal Raj, R. Reghunathan, I. Hubert Joe, V.S. Jayakumar, *J. Raman Spectrosc.* 379 (2006) 1381–1392.
- [19] J.N. Liu, Z.R. Chen, S.F. Yuan, *J. Zhejiang Univ. Sci. B* 6 (2005) 584–589.
- [20] G.S. Kurkcuglu, I. Kavlak, T. Arslan, C. Ogretir, *J. Mol. Model.* 15 (2009) 153–162.
- [21] Mama Nsangou, Nejm–Eddine Jaidane, Zohra Ben Lakhar, *Internet Electron of J. Mol. Des* 5 (2006) 89–101.
- [22] P.L. Anto, Ruby John Anto, Hema Tresa Varghese, C. Yohannan Panicker, Daizy Philipe J. *Raman Spectrosc.* 41 (2010) 113–119.
- [23] T. Sundius, *J. Mol. Struct.* 218 (1990) 321–326.
- [24] (a) T. Sundius, *Vib. Spectrosc.* 29 (2002) 89–95;  
(b) MOLVIB, V.7.0: Calculation of Harmonic Force Fields and Vibrational Modes of Molecules, QCPE Program No.807 (2002)
- [25] J.V. Prasad, S.B. Rai, S.N. Thakur, *Chem. Phys. Lett.* 164 (1998) 629–634.
- [26] Scot H. Brewer, A.M. Allen, S.E. Lappi, T.L. Chase, K.A. Briggman, C.B. Gorman, S. Franzen, *Langmuir* 20 (2004) 5512–5520.
- [27] J. Mohan, *Organic Spectroscopy–Principles and Applications* (2<sup>nd</sup> ed) Narosa Publishing House, New Delhi, P. 30 (2011).
- [28] G. Socrates, *Infrared and Raman Characteristic Group Frequencies*, 3<sup>rd</sup> ed., Wiley, New York (2001).
- [29] V. Krishnakumar, V. Balachandran, *Spectrochim. Acta* 63A (2006) 464–476.
- [30] V. Krishnakumar, R. John Xavier, *Indian J. Pure Appl. Phys.* 41 (2003) 95–98.
- [31] K. Furic, V. Mohacek, M. Bonifacic, I. Stefanic, *J. Mol. Struct.* 267 (1992) 39–44.
- [32] B. Smith, *Infrared Spectral Interpretation, A Systematic Approach*, CRC: Washington DC, (1999).
- [33] D.N. Singh, I.D. Singh, R.A. Yadav, *Ind. J. Phys.* 763 (2002) 307–318.
- [34] G. Varsanyi, R. Arun Balaji, S. Kumaresan, G. Annand, S. Srinivasan, *Canadian Journal of analytical Sciences and Spectroscopy* 53 (2008) 149–162.
- [35] J. Walter, Balfour, *Spectrochim. Acta* 39A (1983) 795–800.
- [36] B. Venkatram Reddy, G. Ramana Rao, *Vib. Spectrosc.* 6 (1994) 231–250.
- [37] N. L. Owen, R.E. Hester, *Spectrochim. Acta* 25A (1969) 343–354.
- [38] G.E. Campangnaro, J.L. Wood, *J. Mol. Struct.* 6 (1970) 117–132.
- [39] V. Krishnakumar, R. John Xavier, *Spectrochim. Acta* 61A (2005) 253–258.
- [40] H.O. Kalinowski, S. Berger, S. Brawn, *Carbon-<sup>13</sup>NMR Spectroscopy*, John Wiley and Sons, Chichester, (1988).
- [41] K. Pihlajer, E. Kleinprter (Eds), *Carbon-<sup>13</sup>Chemical Shifts in Structure and Spectrochemical analysis*, VCH Publishers, Deerfield Beach, (1994).